

Supporting Information

Liquid metal droplet motion transferred from an alkaline solution by a robot arm

Ye Tao, ‡^a Changrui Shi, ‡^a Feiyang Han,^a Ruizhe Yang,^a Rui Xue,^a Zhenyou Ge,^a Wenshang Guo,^a Weiyu Liu,^b Yukun Ren ^{*a}

^a State Key Laboratory of Robotics and System, Harbin Institute of Technology, West Da-zhi Street 92, Harbin, Heilongjiang 150001, People's Republic of China. Email: rykhit@hit.edu.cn

^b Chang'an University, Middle-Section of Nan'er Huan Road, Xi'an 710000, China

This material gives supporting information in the paper:

SI Appendix 1. Design and fabrication information of the robot arm.

SI Appendix 2. Human-computer interaction module of the pose adjustment system.

SI Appendix 3. The visual module of the pose adjustment system.

SI Appendix 4. The hardware part of the modular power transmission system.

SI Appendix 5. The control principle of the robot arm.

SI Appendix 6. Motion analysis of the improved robot arm.

SI Appendix 7. Design and fabrication information of the cargo transportation system.

Supplementary movie:

Movie S1. Three different states of motion.

Movie S2. The demonstration of robot arm moving in different environments.

Movie S3. The demonstration of drawing trajectory.

Movie S4. The demonstration of drawing “W” by the improved robot arm.

Movie S5. The demonstration of cargo transportation function.

Movie S6. The demonstration of glucose concentration detection.

SI Appendix 1. Design and fabrication information of the robot arm

The structural composition of the robot arm is shown in Fig. S1 and the driving units on both sides transmit power to the end-effector in the middle through the connecting rod. The driving units not only support the entire structure but also protect the LMD. The drive unit is designed with a trapezoidal structure, which reduces the overall center of gravity and improves the stability of movement while ensuring that there is enough space on the top to install ceramic bearings. The inner and outer diameters and thicknesses of ceramic bearings are $2\text{ mm} \times 5\text{ mm} \times 2.5\text{ mm}$, which are installed on the top of the driving unit. The robot arm is like an energy transmission medium, which transfers the kinetic energy of the LM from the alkaline solution to the outside world, and completes different tasks according to needs. It is worth mentioning that each driving unit is independent, which can meet different needs by changing the number of it.

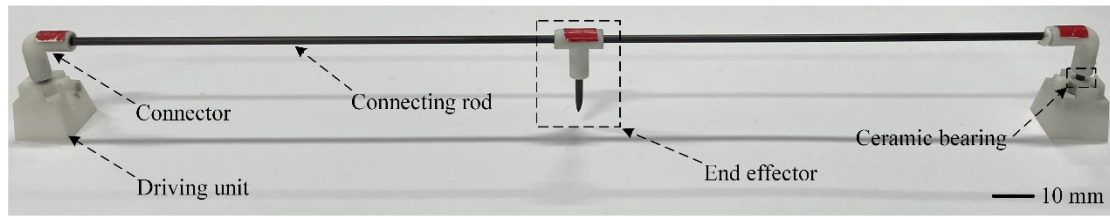


Fig. S1 The physical picture of the robot arm.

The size parameters of the robot arm are shown in Fig. S2, the overall width $a = 150\text{ mm}$, the height of the driving unit $b = 14\text{ mm}$, the height c of the connector, and the steering shaft can be adjusted by replacing the steering shaft of different lengths, the adjustment range is 10 mm - 20 mm , the slope of the side wall $d = 8^\circ$. The total weight of the robot arm is 3.9 g .

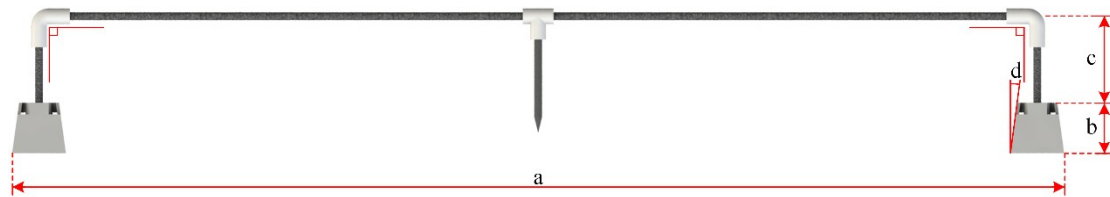


Fig. S2 Front view of the robot arm with related design sizes.

SI Appendix 2. Human-computer interaction module of the pose adjustment system

The human-computer interaction module (HCIM) of the computer is designed by python programming, as shown in Fig. S3. The image captured by the camera is displayed in the upper part of the HCIM in real-time. The lower part of the HCIM is the user interface area, the user can control the opening and closing of the camera and serial port through the corresponding buttons. When the user needs to identify the driving units on both sides, the image detection button can be used to import the target image to be detected, the video can be identified with the visual detection algorithm, and the target can be marked with rectangles of different colors. The detected coordinate information is displayed in the middle part of the HCIM in real-time. According to the different task requirements of users, different functions can be selected to realize the automatic control of the robot arm.

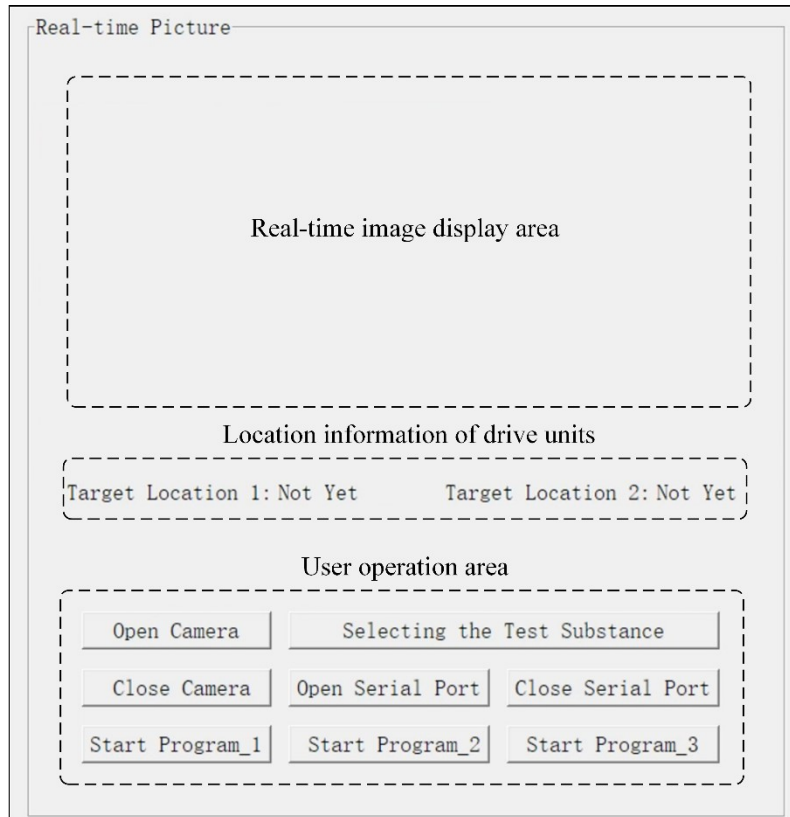


Fig. S3 The human-computer interaction module.

SI Appendix 3. The visual module of the pose adjustment system

The image recognition algorithm used in the vision module is an improved **template-matching** algorithm. Since there are two targets to be identified and they are both inside the corresponding glass container, to improve the accuracy and stability of the recognition, each frame of image in the video stream is segmented, and a rectangular image of the position of the glass container is extracted. The dimension of the rectangular image is 200×200 px, as shown in Fig. S4(b). The template image (Fig. S4(c)) is used as a sliding window to slide in the corresponding rectangular image, then the `cvMinMaxLoc()` function is used to find the position with the highest matching degree, and the rectangular box with different colors is marked, as shown in Fig. S4(d).

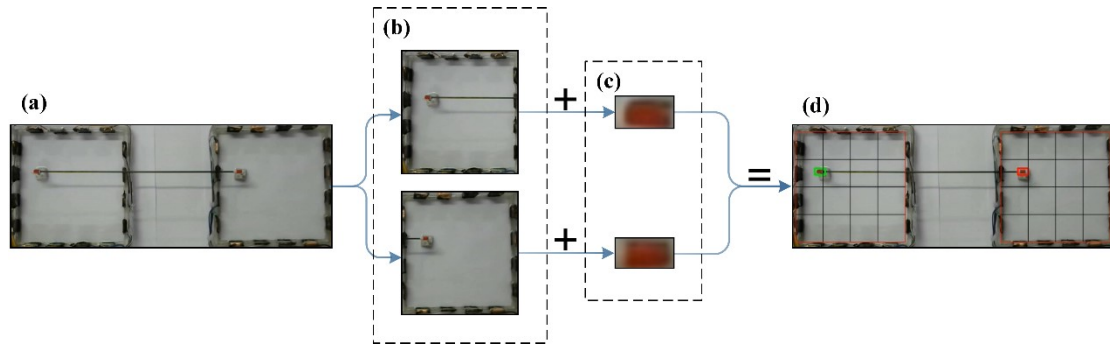


Fig. S4 Principles of visual recognition. (a) The original image to be processed.

(b) The segmented image. (c) The target image to be identified. (d) Visual recognition result.

SI Appendix 4. The hardware part of the modular power transmission system

The hardware composition of the modular power transmission system is shown in Fig. S5(a). As shown in Fig. S5(b), the two driving units of the robot arm are placed in glass containers on both sides, and the middle part is the workspace of the end-effector. Thirty-two graphite electrode sheets are uniformly installed on the side wall of the glass container and connected to the relay module. Four 16-channel relay modules are fixed by copper posts and connected to the MCU by Dupont lines, as shown in Fig. S5(c). The camera is installed on the camera bracket and placed directly above the glass container to collect the real-time position information of the robot arm, as shown in Fig. S5(d). The resolution of the camera is 640×480 px, and the pixel pitch is 0.266 mm. The height of the camera from the desktop is 650 mm, and the visible area is $550 \text{ mm} \times 325 \text{ mm}$.

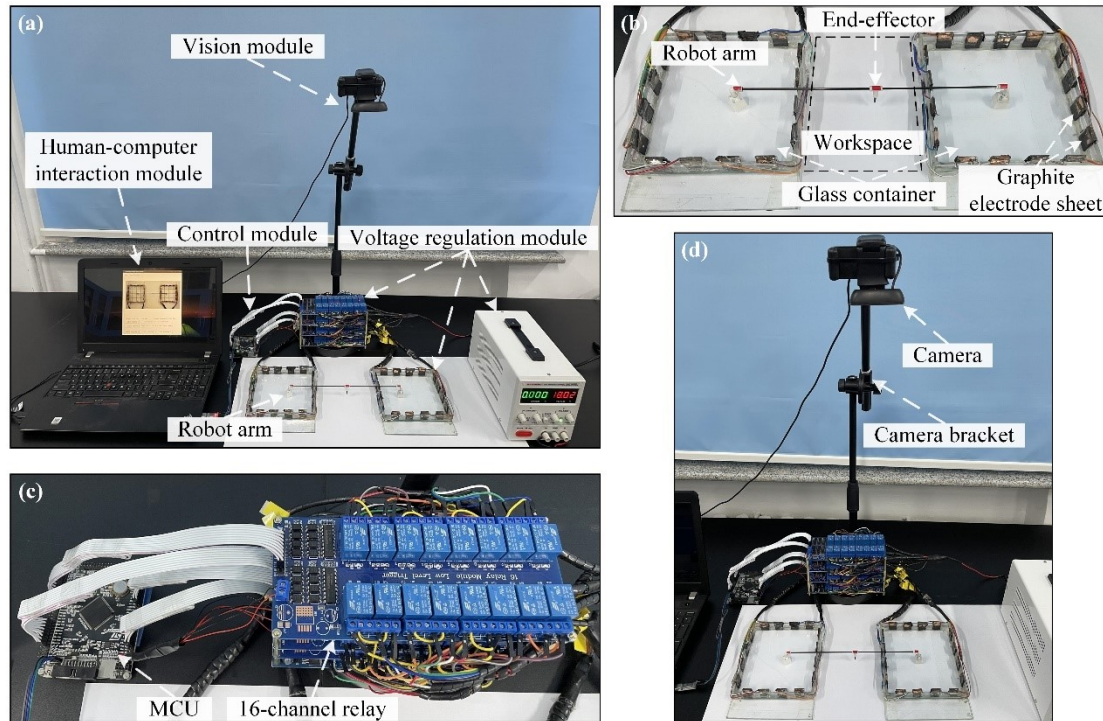


Fig. S5 Composition and description of the overall system.

(a) The physical view of the overall system. (b) Robot arm and its workspace.

(c) Relay modules and MCU. (d) Composition of the visual module.

SI Appendix 5. The control principle of the robot arm

The control module of the robot arm determines the state and position of the activation electrode by comparing the current position with the target position. During the movement, the environment and installation accuracy of the driving units on both sides cannot be guaranteed to be the same, so even though the same electrical signals are applied, the driving units on both sides cannot achieve synchronous movement. Therefore, to improve the synchronization of the robot arm, feedback control is added to the system. When the deviation of the driving units on both sides is large, the driving unit on the side farther from the target position is preferentially driven. To prevent the robot arm from exceeding the target position due to inertia, a fine-tuning interval is set, as shown in Fig. S6(a). When the driving unit enters the fine-tuning range, the voltage regulation module adopts intermittent activation mode to the electrode, which improves the control accuracy.

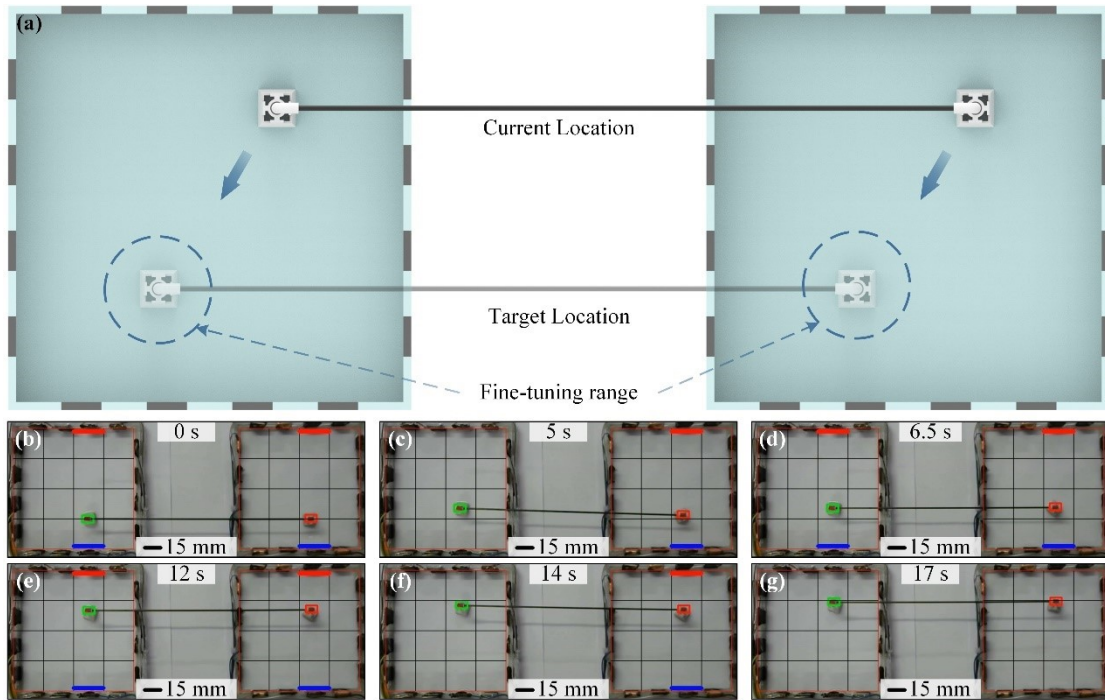


Fig. S6 Robot arm control principle. (a) Schematic diagram of control principle analysis.

(b-g) The sequence diagram of the robot arm moving in a straight line.

The actual application is shown in the sequence diagram of Fig. S6(b-g). When

the robot arm is just started, it is in the synchronous driving stage, and the electrodes on both sides are activated at the same time to drive the robot arm to move, as shown in Fig. S6(b). After moving for 5 s, the right driving unit is slower than the left, so only the right electrode is activated (Fig. S6(c)). At 6.5 s, the robot arm adjusts to the synchronous drive state again (Fig. S6(d)). At 12 s, the robot arm is close to the target position and enters the fine-tuning range (Fig. S6(e)). After 5 s of fine-tuning, the robot arm reaches the target position successfully (Fig. S6(g)).

SI Appendix 6. Motion analysis of the improved robot arm

The original robot arm adopts a single connecting rod for power transmission, and the end-effector has the same motion space as the drive units on both sides, as shown in Fig S7(a). When the improved structure is adopted, the connecting rod is divided into left and right parts. By analyzing the motion space of the left and right connecting rods and taking the intersection, the motion space of the end-effector can be obtained, as shown in Fig S7(b). The motion space of the improved robot arm is 2.2 times that of the original structure.

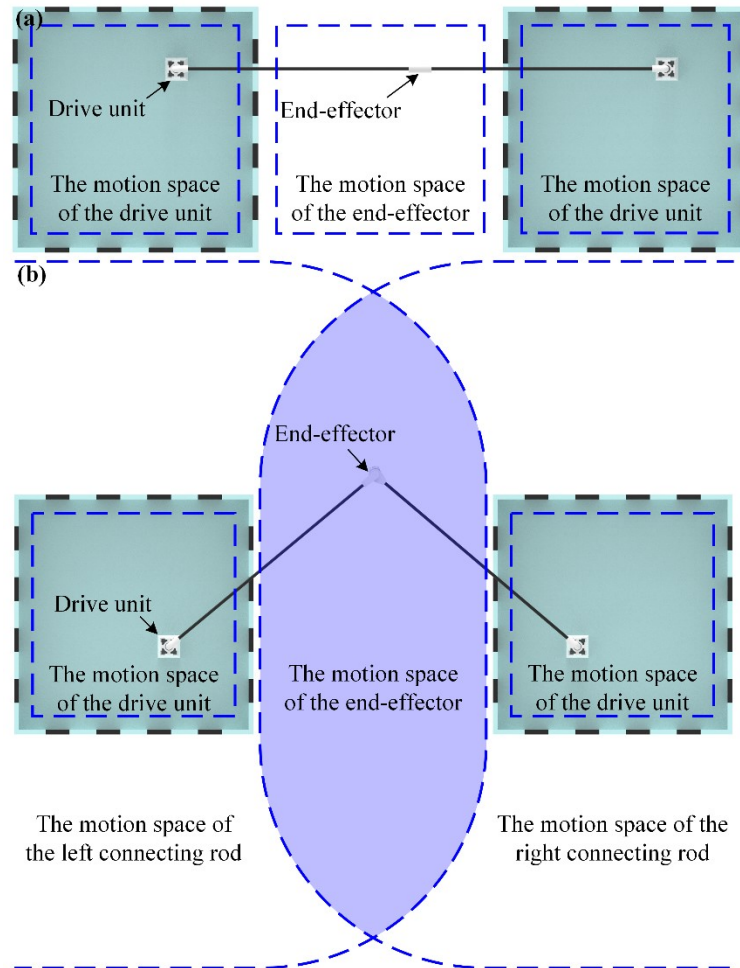


Fig. S7 Motion space analysis of manipulator

SI Appendix 7. Design and fabrication information of the cargo transportation system

The composition of the cargo transportation system is shown in figure Fig. S8. Both the manipulator and the working platform are manufactured by 3D printing technique using photosensitive resin. The size of the working platform used in this experiment is $90\text{ mm} \times 65\text{ mm}$, which can also be adjusted according to requirements. The manipulator is equipped with hand grips in four directions, which can grab the cargo from different directions. The cargo is a 3 mm diameter steel ball, which is placed anywhere on the work platform to simulate the cargo. The circular hole with a diameter of 3.5 mm in the lower left corner of the working platform is the storage area. The manipulator starts from the initial position in the upper right corner, grabs the cargo, and transports them to the storage area to realize the function of cargo transportation.

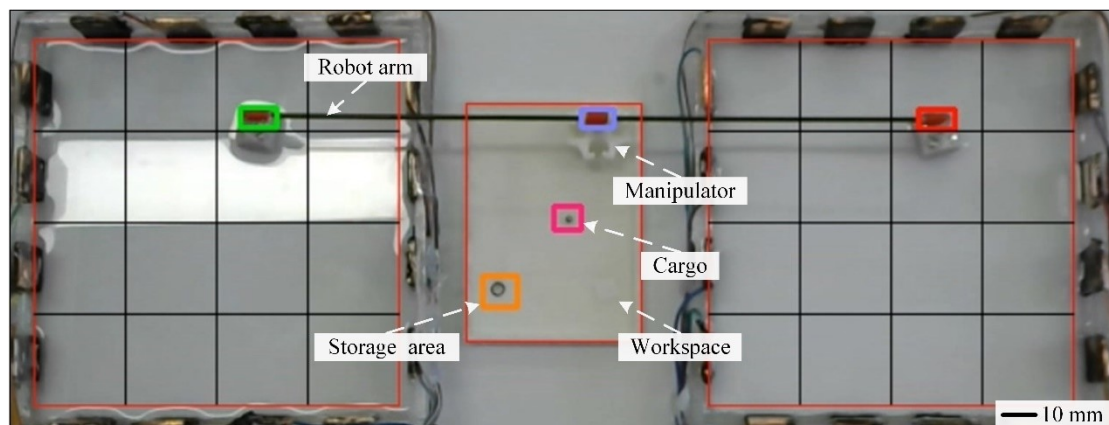


Fig. S8 The composition of the cargo transportation system.